Aromaticity-Controlled Thermal Stability of Photochromic Systems Based on a Six-Membered Ring as Ethene Bridges: Photochemical and Kinetic Studies

ARTICLE *in* CHEMISTRY - A EUROPEAN JOURNAL · SEPTEMBER 2012

Impact Factor: 5.73 · DOI: 10.1002/chem.201200354 · Source: PubMed

6 AUTHORS, INCLUDING:

Yuheng Yang
East China University of Science and Techn…
7 PUBLICATIONS **235** CITATIONS
SEE PROFILE

Weihong Zhu
East China University of Science and Techn…
148 PUBLICATIONS **5,549** CITATIONS
SEE PROFILE

DOI: 10.1002/chem.201200354

Aromaticity-Controlled Thermal Stability of Photochromic Systems Based on a Six-Membered Ring as Ethene Bridges: Photochemical and Kinetic Studies

Yuheng Yang,[a] Yongshu Xie,[a] Qiong Zhang,[a] Keitaro Nakatani,[b] He Tian,[a] and Weihong Zhu*[a]

Abstract: Three photochromic compounds—2-butyl-5,6-bis[5-(4-methoxyphenyl)-2-methylthiophen-3-yl]-1*H*-benzo[*de*]isoquinoline-1,3(2*H*)-dione (BTE-NA), 4,5-bis[5-(4-methoxyphenyl)-2-methylthiophen-3-yl]benzo[*c*]-[1,2,5]thiadiazole (BTA), and BTTA, which contain naphthalimide, benzothiadiazole, and benzobisthiadiazole as six-membered ethene bridges with different aromaticities—were systematically studied in solution, sol–gel, and single-crystal states. They exhibit typical photochromic performance with considerably high cyclization quantum yields. BTE-NA, BTA, and BTTA form a typical donor–π–acceptor (D–π–A) system with significant intramolecular charge transfer (ICT) between HOMO and LUMO upon excitation, thus realizing the fluorescence modulation by both photochromism and solvatochromism. The three ethene bridges with different degrees of aromaticity can provide a systematic comparison of the thermal stability evolution for their corresponding closed forms (c-BTE-NA, c-BTA, and c-BTTA). c-BTE-NA shows first-order decay in various solvents from cyclohexane to acetonitrile. c-BTA only shows first-order decay in polar solvents such as chloroform, whereas it is stable in nonpolar solvents like toluene. In contrast, the less aromatic property of BTTA gives rise to its unprecedented thermal stability in various solvents even at elevated temperatures in toluene (328 K). Moreover, the small energy barrier between the parallel and antiparallel conformers allows the full conversion from BTTA to c-BTTA. In well-ordered crystal states, all three compounds adopt a parallel conformation. Interestingly, BTTA forms a twin crystal of asymmetric nature with interactions between the electron-rich oxygen atom of the methoxy group and the carbon atom of the electron-deficient benzobisthiadiazole moiety. This work contributes to the understanding of aromaticity-controlled thermal stability of photochromic systems based on a six-membered ring as an ethene bridge, and a broadening of the novel building blocks for photochromic bisthienylethene systems.

Keywords: aromaticity · benzobisthiadiazoles · charge transfer · diarylethenes · photochromism

Introduction

Research on photochromic systems has received much attention over the past two decades on account of their distinguishable absorption spectra in two different states and their potential applications in ophthalmic lenses, smart molecular materials in which they act as photoresponsive self-assemblies, molecular switches, logic gates, and information storage.[1] In particular, bisthienylethenes (BTEs) have attracted much more attention on account of their thermal irreversibility and outstanding fatigue resistance among various photochromic systems, in which the 1,3,5-hexatriene section could adopt an appropriate conformer to undergo conrotatory 6π-electron photocyclization upon excitation with UV light.[2] To date, most studies have focused on molecular design, especially the symmetric and asymmetric synthesis of organic frameworks in diarylethenes with different heteroaryl units such as thiophene or benzothiophene, furan and benzofuran, thiazole, indole, pyrazole, and pyrrole rings.[3] However, exploitation of the central ethene bridge has been confined to a cyclopentene unit or its strong electron-withdrawing analogues, such as perfluorocyclopentene, maleic anhydride, or maleic imide.[4] Alternatively, several groups have chosen six-membered rings as a BTE central bridge to perform photochromism. For instance, Yam and co-workers took advantage of the complexation ability of the 1,10-phenanthroline ligand to form the backbone of a novel diarylethene photochromic complex, which was utilized to tune the excitation wavelength and photochromic behavior.[5] Yokoyama and co-workers exploited the fluores-

[a] Y. Yang, Prof. Dr. Y. Xie, Dr. Q. Zhang, Prof. Dr. H. Tian, Prof. Dr. W. Zhu
Shanghai Key Laboratory of Functional Materials Chemistry
Key Laboratory for Advanced Materials and Institute of Fine Chemicals
East China University of Science and Technology
Shanghai 200237 (P.R. China)
Fax: (+86) 21-6425-2758
E-mail: whzhu@ecust.edu.cn

[b] Prof. Dr. K. Nakatani
PPSM, ENS Cachan, CNRS, UniverSud
61 av Président Wilson, 94230 Cachan (France)
Fax: (+33) 1 47402454

Supporting information for this article is available on the WWW under http://dx.doi.org/10.1002/chem.201200354.

cence property of coumarin to construct a functional ethene bridge, thus achieving dual-mode fluorescence switching.[6]

On the other hand, on account of the strong aromaticities of six-membered ethene bridges, the greatly enhanced ground-state energy difference (Hückel rule) between the open and closed forms ultimately results in the thermal instability of the closed form in BTEs.[7] With this in mind, we have recently synthesized a novel photochromic BTE system based on the specific benzobisthiadiazole unit that shows excellent thermal stability for the closed form in various solvents from nonpolar to polar, and even at elevated temperatures.[8] Since the ethene bridge with a six-membered ring has its own advantages such as a higher quantum yield on ring closure and longer absorption wavelength, we envision that the six-membered ring with low or non-aromaticity as the center ethene bridge might greatly extend the diversity of the thermally irreversible photochromic systems. However, up to now, insight into the ethene bridges has seldom been provided. Accordingly, we systematically report herein the synthesis and photochromic properties of three ethene bridges with different degrees of aromaticity (2-butyl-5,6-bis[5-(4-methoxyphenyl)-2-methylthiophen-3-yl]-1*H*-benzo[*de*]isoquinoline-1,3(2*H*)-dione (BTE-NA), 4,5-bis[5-(4-methoxyphenyl)-2-methylthiophen-3-yl]benzo[*c*][1,2,5]thiadiazole (BTA), and BTTA; Scheme 1), which is expected to achieve clear thermal stability evolution, and realize the fluorescence modulation by solvato- and photochromism in the six-membered ethene-bridged photochromic systems. As expected, an extremely low aromatic property of the center ethene bridge with a benzobisthiadiazole unit ultimately leads to the unexpected thermally irreversible photochromic system (BTTA). Moreover, the small energy barrier between the parallel and antiparallel conformers allows the full conversion from BTTA to c-BTTA. For the first time, the three ethene bridges with different degrees of aromaticity provided a systematical comparison of the thermal-stability evolution of their corresponding closed forms. This work contributes to the understanding of aromaticity-controlled thermal stability of photochromic systems based on six-membered rings as ethene bridges, and broadens the novel building blocks for photochromic BTE systems.

Results and Discussion

Molecular design and synthesis: Naphthalimide, benzothiadiazole, and benzobisthiadiazole are excellent candidates for acceptor moieties on account of their attractive photophysical properties and their priority in electron-withdrawing capabilities. As shown in Scheme 1, we designed novel BTE derivatives with these building blocks based on the following points: 1) given the similarly strong electron-withdrawing properties of perfluorocyclopentene, maleic anhydride, or maleic imide, the remarkable electron-withdrawing units of naphthalimide, benzothiadiazole, and benzobisthiadiazole are supposed to assure good photochromism with considerable bistability, high cyclization quantum yield, and fatigue resistance; 2) naphthalimide, benzothiadiazole, and benzobisthiadiazole are essentially well-known fluorescent build-

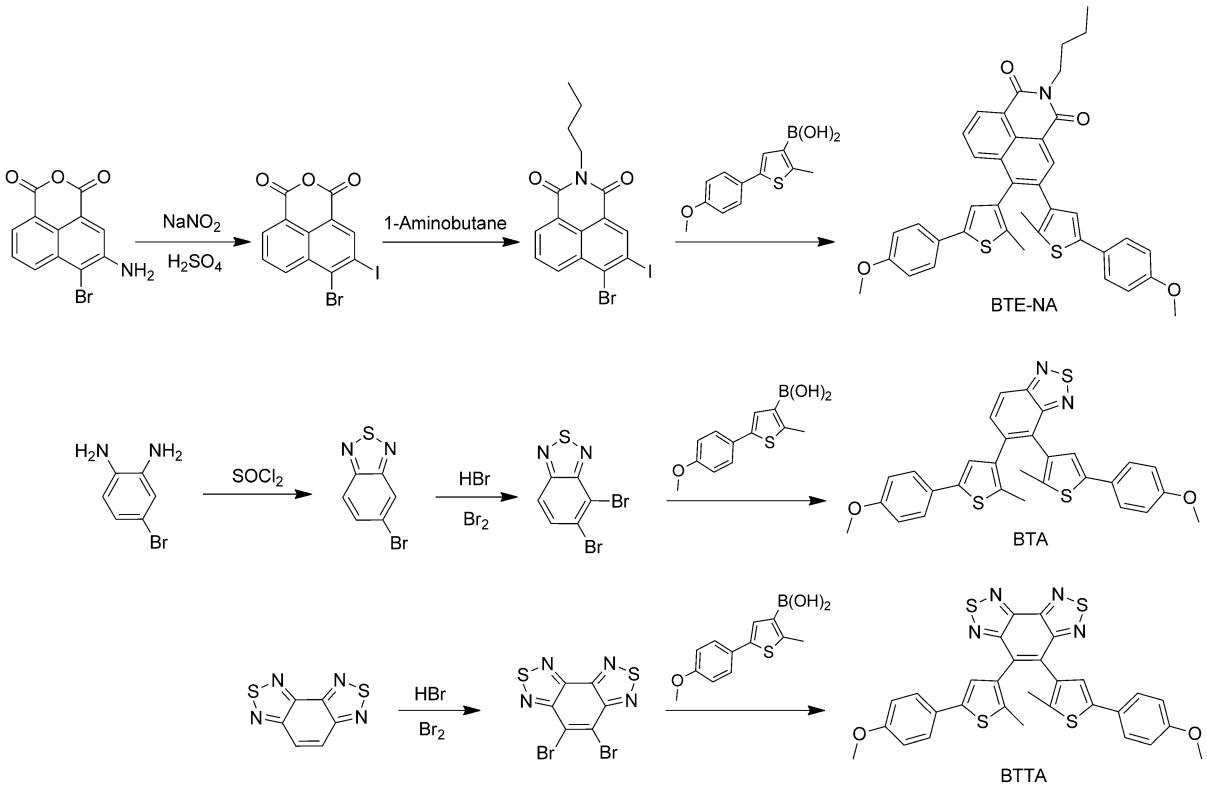

Scheme 1. Synthetic routes to BTE-NA, BTA, and BTTA.

ing blocks in the design of functional materials such as sensors, OLEDs, nonlinear optics (NLO), and solar cells.[9] Thus, the electron-withdrawing groups and the electron-donating anisole can form an efficient donor–π–acceptor (D–π–A) system with significant charge transfer between HOMO and LUMO upon excitation to realize the fluorescence modulation by means of both photochromism and solvatochromism;[10] and 3) the three ethene bridges with different degrees of aromaticity can provide a systematical comparison of the thermal stability evolution for their corresponding closed forms.

Scheme 1 summarizes the synthetic routes to BTE-NA, BTA, and BTTA in this study. 5-(4-Methoxyphenyl)-2-methylthiophen-3-ylboronic acid was prepared by the reported procedure[11] and was used as a building block to synthesize the desired target molecules. The key intermediates of 4-bromo-*N*-butyl-3-iodo-1,8-naphthalimide,[11] 4,5-dibromo-2,1,3-benzothiadiazole,[12] and 4,5-dibromobenzo[1,2-*c*:3,4-*c*′]bis[1,2,5]thiadiazole[8] were conveniently synthesized from 4-bromo-1,8-naphthalic anhydride, 4-bromobenzene-1,2-diamine, and benzothiadiazole,[13] respectively. The Suzuki coupling between 4-bromo-*N*-butyl-3-iodo-1,8-naphthalimide, 4,5-dibromo-2,1,3-benzothiadiazole, 4,5-dibromobenzo[1,2-*c*:3,4-*c*′]bis[1,2,5]thiadiazole, and 5-(4-methoxyphenyl)-2-methylthiophen-3-ylboronic acid in the presence of a $[Pd(PPh_3)_4]$ catalyst in a mixture of aqueous Na_2CO_3 (2 M) and 1,4-dioxane under reflux conditions gave the target molecules of BTE-NA, BTA, and BTTA, which were fully characterized by ^1H and ^{13}C NMR spectroscopy as well as high-resolution MS (HRMS; shown in the Experimental Section and the Supporting Information).

Optical properties and photochromism: All three compounds were found to easily dissolve in toluene to give a colorless solution without any absorption bands in the visible range. In general, the electronic absorption spectra for the open forms of BTE-NA, BTA, and BTTA in toluene at 298 K show an intense absorption band in the range of 290–350 nm and a moderately intense band at 378–430 nm (Figure 1). Upon UV irradiation at 365 nm, the corresponding closed forms (c-BTE-NA, c-BTA, and c-BTTA) were produced by the typical photocyclization as the colorless solution changed to yellow green, bright green, and then dark green, respectively, thereby resulting in broad absorption bands centered at 719 (c-BTE-NA), 657 (c-BTA), and 497 and 655 nm (c-BTTA). The significant difference in absorption bands of the closed forms compared to their open forms is mainly due to the increase in π conjugation, which dramatically changes the electronic structure as a whole in such a way that new electronic transitions are observed in the visible region. The longer wavelength of c-BTE-NA in the visible region than that of c-BTTA strongly indicates that the energy gap between the HOMO and LUMO orbitals of c-BTE-NA is smaller than that of c-BTTA, which results from the strong conjugation between 2-(4-methoxyphenyl)-5-methylthiophene and *N*-butyl-1,8-naphthalimide units. The typical photochromic properties of BTE-NA,

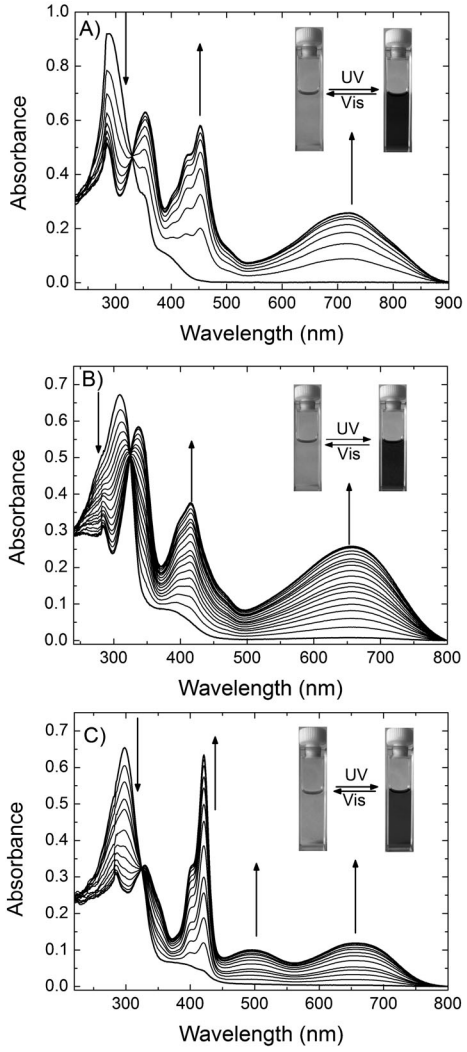

Figure 1. Absorption changes upon irradiation at 365 nm: A) BTE-NA in toluene (2.31×10^{-5} mol L^{-1}); B) BTA in toluene (1.85×10^{-5} mol L^{-1}); C) BTTA in toluene (1.14×10^{-5} mol L^{-1}). The corresponding inset photographic images are BTE-NA (2.31×10^{-4} mol L^{-1}), BTA (1.85×10^{-4} mol L^{-1}), and BTTA (1.14×10^{-4} mol L^{-1}) in toluene upon irradiation at 365 nm.

BTA, BTTA and their corresponding closed forms (c-BTE-NA, c-BTA, and c-BTTA) are summarized in Table S1 in the Supporting Information. Notably, the ring-closure quantum yield of these three ethene bridges decreased with the loss of aromaticity. The ring-closure quantum yields for BTE-NA, BTA, and BTTA are 43.13, 38.21, and 10.96% in cyclohexane, respectively. This might be ascribed to the competition between different pathways to the ground state. The fluorescence quantum yields for BTE-NA, BTA, and BTTA were found to be 0.76, 0.12, and 0.48% in cyclohexane, respectively. The extremely low fluorescence quantum yield is indicative of the inefficient radiative pathway to the ground state. Accordingly, the excited molecules could be predominately deactivated through photocyclization or other nonradiative approaches. Here the decrease in photocyclization quantum yield for BTTA is probably the result

of the increased spin–orbit coupling and possible triplet decay due to the increased inclusion of sulfur atoms in the ring systems.

NMR spectroscopic changes before and after irradiation: In fact, distinct ^{1}H NMR spectroscopic changes could be observed in photochromic systems due to the large chemical environment changes between the open and closed forms. The ^{1}H NMR spectra of BTE-NA and BTA show only one set of signals for the methyl protons on thiophene rings located at $\delta = 1.82$ and 2.13 ppm for BTE-NA and $\delta = 1.98$ and 2.03 ppm for BTA in [D_6]benzene (Figure S1 in the Supporting Information). The different chemical shifts of the two methyl protons are only on account of the asymmetric organic framework of the central ethene bridge. However, the ^{1}H NMR spectrum of BTTA in [D_6]benzene shows two well-resolved sets of signals for the methyl protons that correspond to the parallel ($\delta = 2.04$ ppm) and antiparallel ($\delta =$ 1.98 ppm) conformers (Figure 2). In fact, the two conformations—parallel (photochromic inactive) and antiparallel (photochromic active) conformers—undergo very fast single-bond rotation in BTE-NA and BTA, thereby resulting in only one set of time-averaged signals in the ^{1}H NMR spectra. Only in the cases of BTEs with large energy barriers between two conformers can the rotation of the aryl groups be slowed down sufficiently to give two sets of signals.[7] As found by the area integration in ^{1}H NMR spectra (Figure 2), the ratio between the parallel and antiparallel conformers of BTTA in [D_6]benzene is 64:36. When irradiated at 365 nm, the open form was converted to the closed form (c-BTTA) with absorption bands in the visible region. The existence of c-BTE-NA, c-BTA, and c-BTTA could also be evidenced by ^{1}H NMR spectroscopy. For BTE-NA (Figure S1A in the Supporting Information), the signals of H_a, H_b, and H_c on the butyl group after photocyclization (in [D_6]benzene) do not show any obvious changes with respect to the open form due to the distance far away from the π-delocalization of naphthalimide, whereas the methylene hydrogen signals (H_d) attached to the imide nitrogen shift by 0.07 ppm from $\delta = 4.37$ to 4.30 ppm. The two groups of methyl protons (H_o, H_p) on the thiophene ring in BTE-NA shift from $\delta = 1.82$ and 2.13 ppm to $\delta = 2.37$ and 2.50 ppm, respectively. There is a similar case for the two methyl protons (H_i, H_j) on the thiophene group of BTA (in [D_6]benzene), which shift downfield from $\delta = 1.98$ and 2.03 ppm to $\delta = 2.46$ and 2.50 ppm, respectively (Figure S1B in Supporting Information).

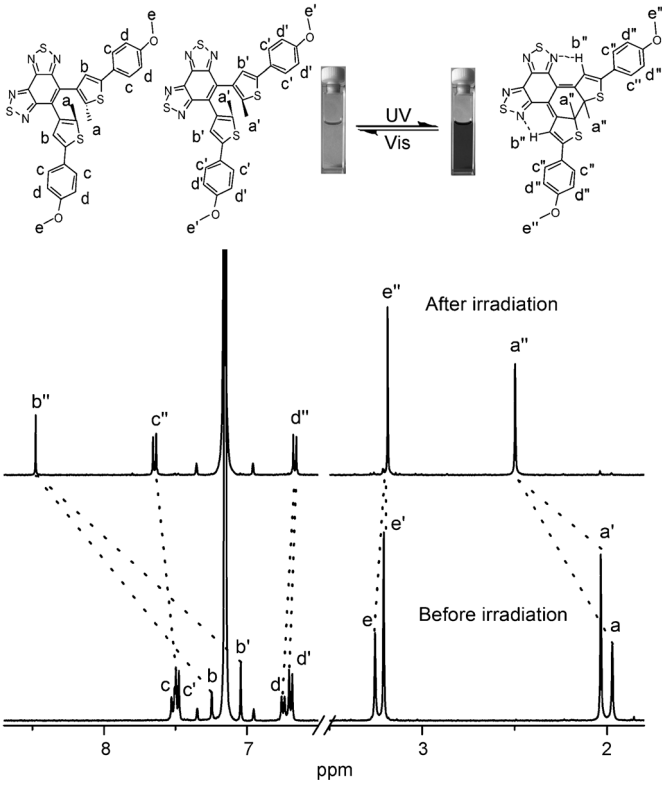

Figure 2. ^{1}H NMR spectroscopic changes of BTTA in [D_6]benzene. Note: the inset photographic images were taken of BTTA in toluene (1.14×10^{-4} mol L^{-1}) upon irradiation at 365 nm.

Generally speaking, the proton resonances on the thiophene heterocycles and six-membered ethene bridges shift upfield upon ring-closure of diarylethene,[14] which is due to the aromaticity loss of heterocycles in the ring-closure reaction. In the ring-open form, the resonances of the protons attached to thiophene units and six-membered rings appear in the ^{1}H NMR spectroscopic aromatic region. In contrast, the resonances for these protons in the ring-closed form appear in the region characteristic of alkenes. As expected, after the ring closure of BTE-NA upon irradiation at 365 nm, the aromaticity of the naphthalimide and thiophene groups is disturbed, and the protons (H_e, H_f, H_g, and H_h) on the naphthalimide moiety shift remarkably to the high field upon photocyclization (Figure S1A in the Supporting Information). A typical triplet peak that corresponds to H_f moves from $\delta = 7.14$ to 6.98 ppm. The singlet peak of H_h shifts significantly from $\delta = 8.91$ to 8.24 ppm. Additionally, the two protons (H_i and H_v) located on thiophene are $\delta = 6.94$ and 6.84 ppm for BTE-NA, whereas they shift to $\delta = 6.86$ and 6.61 ppm after photocyclization. Similarly in the case of BTA, the chemical shifts of H_a and H_b on the benzothiadiazole (BTA) and H_c move to high field (Figure S1B in the Supporting Information). Interestingly, in contrast to the two protons (H_c and H_p) located on thiophene ($\delta = 6.95$ and 7.16 ppm) for BTA, H'_c shifts upfield to $\delta = 6.39$ ppm, whereas H'_p shifts downfield to $\delta = 8.43$ ppm for c-BTA. Also in the system of BTTA, the protons of H_b and H'_b on the thiophene rings of BTTA shift downfield from $\delta = 7.05$ and 7.25 ppm in the open form to $\delta = 8.48$ ppm after photocyclization (Figure 2). The dramatic downfield shifts of H'_p for BTA could be attributed to the possible formation of an intramolecular hydrogen bond between H'_p and the N atom on the benzothiadiazole moiety (Figure S1B in the Supporting Information). Similarly, the intramolecular hydrogen bonds between H_b, H'_b, and the N atom on the benzobisthiadiazole units ultimately lead to the downfield shift of H_b and H'_b upon photocyclization (Figure 2).

Interestingly, in case of BTTA (in [D_6]benzene), the two sets of well-resolved proton signals on the thiophene and methyl groups of methoxy on the phenyl rings are converted into one set of proton signals (they move from $\delta = 1.98$ and 2.04 to 2.50 ppm; $\delta = 3.22$ and 3.26 to 3.19 ppm, respectively). It is the same case for the protons on phenyl rings after photocyclization. The simultaneous disappearance of the two sets of signals indicates that a slow interconversion between parallel and antiparallel conformations takes place in the system, and that the chemical environment of the two sets of methyl groups becomes identical after photocyclization. It might be due to the small energy barrier between the parallel and antiparallel conformers of BTTA and c-BTTA in the absorption spectra that allows the full conversion from BTTA to *c*-BTTA as demonstrated in the ^{1}H NMR spectra (Figure 2).

Fluorescence modulation and solvatochromism: As shown in Table S1 in the Supporting Information, the absorption bands of the open and closed forms in various solvents remain in the range of 378–430 nm and 650–719 nm, thus indicating that the solvent dependence of the absorption band is rather small according to the Franck–Condon principle. All three compounds show noticeable fluorescence, which could be sufficiently modulated by solvato- and photochromism. Indeed, upon excitation at 719 (BTE-NA), 657 (BTA), and 655 nm (BTTA), no significant fluorescence signals could be recorded from the closed form. The fluorescence quenching in the photostationary state (PSS) in toluene is 77% for BTE-NA, 92% for BTA, and 94% for BTTA (excited at the isobestic points of 329, 324, and 324 nm, respectively), which are fully compatible with the conversion yield (Table S1 in the Supporting Information). Thus, the fluorescence quenching of BTE-NA, BTA, and BTTA is simply due to the disappearance of the open form upon photocyclization and the nonfluorescent property of the corresponding closed form (Figure 3A and Figures S3–S5 in the Supporting Information). Moreover, the solvent polarity plays a decisive role in the emission wavelength on account of the strong electron-withdrawing nature of naphthalimide, benzothiadiazole, and benzobisthiadiazole, and the moderate electron-donating ability of anisole rings. When the three compounds were excited, the dipole moment was largely enhanced for all of them. In nonpolar solvents like cyclohexane, the dipolar moments could not be stabilized, and hence, the emission wavelength was shorter. In polar solvents like acetonitrile, however, the stabilized dipolar moment yielded a small energy gap between the HOMO and LUMO, and thus a longer emission wavelength was observed (Figure 3B). The peak of the emission bands appear at 464 and 601 nm in cyclohexane and THF for BTE-NA, 494 and 670 nm in cyclohexane and acetonitrile for BTA, and 488 and 636 nm in cyclohexane and acetonitrile for BTTA, respectively (Tables S2–S4 in the Supporting Information). Clearly, the solvatochromism of all three compounds arises from the possible photoinduced charge transfer from the donor anisole group to the electronegative central ethene bridge. The positive linearity of the Lippert–Mataga plots also illustrates that there is a higher dipole moment in the excited state than in the ground state (Figure S6 in the Supporting Information).

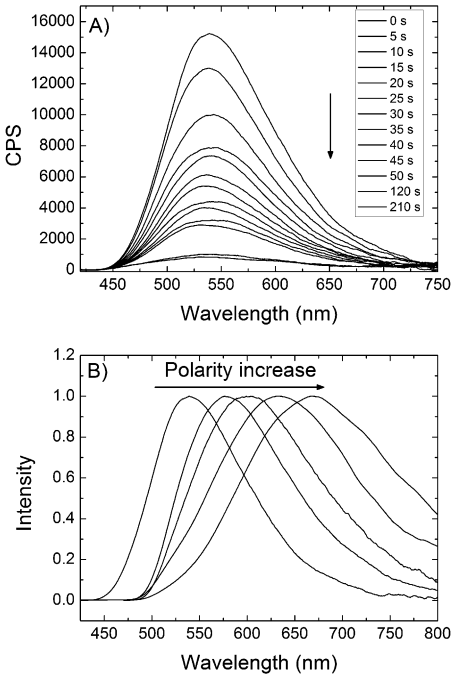

Figure 3. A) Fluorescence spectral changes of BTA in toluene with the excitation at isobestic point 324 nm. B) Normalized fluorescence spectra of BTA in various solvents (from left to right: cyclohexane, toluene, THF, chloroform, acetone, and acetonitrile).

Effects of the ethene bridge on the thermal stability of the closed forms in various solvents: The energy barrier, which correlates to the ground-state energy difference between the open and the closed forms, contributes to the stability of the photogenerated closed-ring isomers. In fact, the change in aromatic character of the six-membered ethene from its open to closed form during the course of photocyclization can control the ground-state energy difference. With the strong aromaticity of the central ethene bridge, the energy barrier for the cycloreversion thus becomes smaller. Hence, the thermal back-reaction is ready to take place.[7] As expected, c-BTE-NA is unstable even at 293 K due to the large difference in the ground-state energy before and after irradiation. As illustrated in Table 1, the absorbance at around 710 nm for BTE-NA could be completely bleached

Table 1. Spectrokinetic data of thermal bleaching for BTE-NA in various solvents at 293 K.[a]

Solvents	λ_{max} [nm]	$\tau_{1/2}$ [s]	k [10^{-3} s^{-1}]	A_0
cyclohexane	708	647.5	1.01	0.863
toluene	717	581.4	1.27	0.919
THF	716	215.3	3.10	0.660
acetonitrile	719	182.2	3.71	0.150

[a] The values k and A_∞ are the fitted parameters from Equation (1); λ_{max}, $\tau_{1/2}$, and A_0 were obtained from the experimental data.

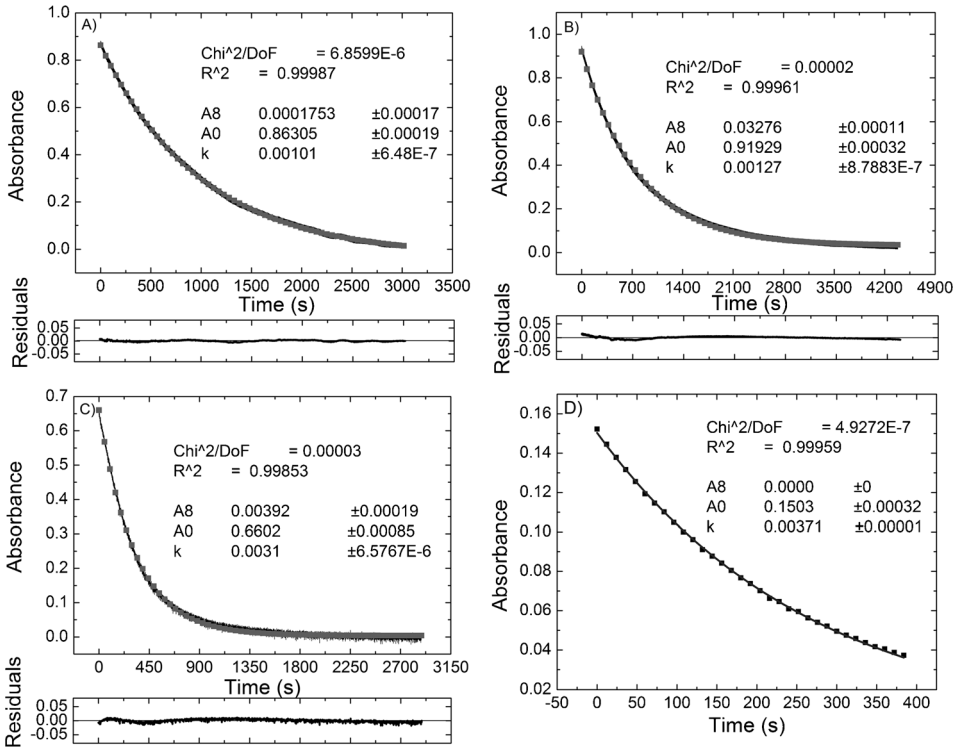

Figure 4. The monoexponential (first-order) decay model and experimental thermal fading kinetics of BTE-NA monitored at 708, 717, 716, 719 nm in A) cyclohexane (8.67×10^{-5} mol L^{-1}), B) toluene (8.26×10^{-5} mol L^{-1}), C) THF (6.23×10^{-5} mol L^{-1}), and D) acetonitrile (1.43×10^{-5} mol L^{-1}) at 293 K, respectively (black line: data measured; gray dot: the first-order decay model fitted; solid line: the absorbance residuals at testing time). Inset: the first-order decay model parameters. Note: Due to the fast bleaching rate of BTE-NA in acetonitrile and low signal-to-noise ratio, the experiment of picture D was carried out on a CARY instrument in scanning kinetic mode. Thus the residuals were omitted due to the small amount of data points.

within 35 min, thereby indicating the great loss of aromaticity after the photocyclization reaction. The thermal back-reaction rates for c-BTE-NA are 1.01×10^{-3}, 1.27×10^{-3}, 3.10×10^{-3}, and 3.71×10^{-3} s^{-1} in cyclohexane, toluene, THF, and acetonitrile, respectively, as monitored by using a charge-coupled device (CCD) camera mounted on a spectrometer and on a CARY instrument in the kinetic mode (Figure 4). More impressively, the decay becomes much faster in chloroform (1.80×10^{-1} s^{-1}; Table 2). The experimental data were fitted with Equation (1),[15] in which A_0, A_∞, and A are the initial absorbance, infinite absorbance, and absorbance at τ(s), respectively.

$$k\tau = -\ln[(A-A_\infty)/(A_0-A_\infty)] \quad (1)$$

Generally, the decrease in aromaticity can greatly increase the bistability of the BTE system. On account of the decrease in aromaticity, c-BTA shows no clear thermal back-reaction in nonpolar solvents like toluene, even at 328 K. However, c-BTA is not stable in polar solvents such as chloroform, which was found to follow similar first-order decay with a constant of 1.52×10^{-5} s^{-1} (Figure S7 in the Supporting Information), four magnitudes slower than that of BTE-NA (1.80×10^{-1} s^{-1}). As shown in Figure 5 and Table 2, BTA exhibits first-order decay in chloroform with a half-life ($\tau_{1/2}=4.58\times10^{4}$ s) much slower than that of BTE-NA (3.89 s). The different thermal back-reaction rates in the system of BTE-NA and BTA are apparently on account of the difference in activation energy of the thermal cycloreversion in various solvents.

Table 2. Spectrokinetic data of thermal bleaching for BTE-NA, BTA, and BTTA in chloroform at 293 K

	λ_{max} [nm]	$\tau_{1/2}$ [s]	k [s^{-1}]	A_0
BTE-NA	719	3.89	1.80×10^{-1}	0.28
BTA	657	4.58×10^{4}	1.52×10^{-5}	1.63
BTTA	655	–[a]	–[a]	0.87

[a] Data could not be obtained.

In contrast, no obvious thermal back-reaction could be observed for BTTA in the dark and 273 K for a prolonged time. As a matter of fact, BTTA preserves very promising thermal stability with almost flat decays, and does not show any thermal back-reaction in various solvents like cyclohexane, toluene, chloroform, and even in acetonitrile in the dark and 293 K (Figures S8–S10 in the Supporting Information). Even the pure closed form was successfully separated on aluminum oxide eluted with CCl_4 and dichloromethane (volume ratio 4:1; Figure S25 in the Supporting Information). At elevated temperatures (328 K) in toluene, BTTA does not show any obvious decrease in its absorbance at 655 nm after 800 min (Figure S9 in the Supporting Information).

Furthermore, the absorption bands of BTTA in the visible region could be gradually bleached as a result of the photochromic back-reaction upon irradiation at 575 nm, thus showing a typical photoresponsive back-reaction. However, for BTE-NA and BTA, the photochromic reaction could be reverted either by thermal back-reaction in the dark in polar solvents or upon irradiation at 575 nm. Thus, considering the high polarity and electron-withdrawing tendency of the benzobisthiadiazole unit, the incorporation of an extremely highly polar, low aromatic unit with benzobisthiadiazole as the center ethene bridging unit can ultimately lead to a thermally irreversible photochromic system that can even be comparable to the photochromic performances of parent BTEs, such as the widely known five-membered hexafluorocyclopentene-based counterparts.

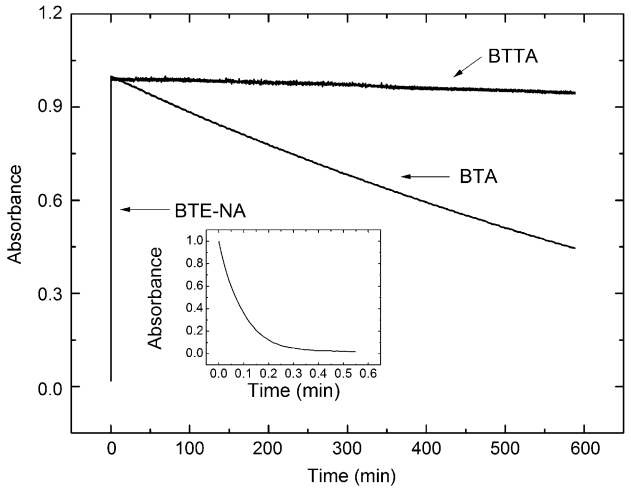

Figure 5. Thermal back-reaction of BTE-NA, BTA, and BTTA in chloroform at 293 K. Inset: the enlarged graph is the thermal back-reaction of BTE-NA in chloroform at 293 K.

Theoretical calculations: To gain further insight into the aromaticity-controlled thermal stability, the calculations were performed with the Gaussian 09 program.[16] The geometries were optimized with the Perdew–Burke–Ernzerhof (PBE0) functional[17] and the 6-31G(d,p) basis set. The energies obtained from the small basis-set optimizations are not accurate enough. On the basis of the optimized structures, more accurate energies can be achieved by performing single-point calculations with the larger 6-311+G(d,p) basis set. The solvent effect is taken into account within the polarizable continuum model (PCM)[18] in the single-point calculations.

For BTTA, BTA, and BTE-NA, the open-ring isomers are more stable than the closed-ring isomers both under vacuum and in solvents. Destabilization on account of the destruction of the aromatic thiophene rings and central ethene bridges during the course of cyclization increases the ground-state energy of the closed-ring isomers.[7] In BTE derivatives, the cycloreversion reaction in the ground states generally has to overcome the energy barriers that correlate to the ground-state energy differences. The calculated values of ground-state energy difference between the open and closed isomers for BTTA, BTA, and BTE-NA are −4.93, −10.16, and −20.44 kcal mol^{-1} under vacuum, respectively (Tables S5 and S6 in the Supporting Information). When the ground-state energy difference is large, the energy barrier becomes small and the cycloreversion reaction readily takes place. On the other hand, the reaction barrier becomes large when the ground-state energy difference is small. In the case of c-BTTA, the cycloreversion reaction could not occur easily in the ground state relative to c-BTE-NA and c-BTA. Accordingly, the destabilization energy, which correlates to the decrease in aromaticity during the course of photocyclization, is lower in BTTA than in BTA, and much lower than in BTE-NA. The small energy difference between the open and closed forms results in the excellent thermal stability of c-BTTA in a variety of solvents.

BTE-NA, BTA, and BTTA in the single-crystal state and organogel systems: Single crystals of the open forms of BTE-NA, BTA, and BTTA were grown by slow evaporation of the corresponding solutions in mixed solvents of THF/MeOH, THF/H_2O, and $CHCl_3$/MeOH, respectively. X-ray crystal-structure analyses revealed that in all these crystals only parallel conformations are observed, thereby indicating that all three of these systems cannot undergo photocyclization in the single-crystal state. For the crystal of BTE-NA (Figure S11 in the Supporting Information), two molecules are arranged in a head-to-tail fashion to afford a dimeric moiety by the intermolecular C−H···O hydrogen bonds with H···O distances of 2.43 Å, and C−H···O angles of 174°. Interestingly, weak O···C interactions are observed between naphthalimide and methoxy units, with O···C distances of 3.120(2) Å, which is smaller than the sum of the van der Waals radii for O and C atoms. These interactions might be understood as electrostatic interactions between the electron-rich O atom and the electron-deficient naphthalimide carbon atom. For the crystal of BTA (Figure 6), multiple intermolecular C−H···O hydrogen bonds are found that involve the methoxy O atoms and phenyl C−H moieties, with H···O distances of 2.48 Å and C−H···O angles of 160°. Thus, interesting supramolecular linear structures are formed by these interactions.

For the crystal of BTTA (Figure 7), S···π interactions are observed with the shortest S···C distances of 3.412(5) Å. Similar to that observed in the crystal of BTE-NA, weak O···C interactions are also observed between benzobisthiadiazole and methoxy units, with O···C distances of 3.12(5) Å. Thus, a linear structure is formed by these interactions (Figure 7c). From these observations, it is reasonable to assert that the multiple intermolecular interactions stabilize and fix the conformations of the molecules. Thus, only the parallel conformations are observed. In contrast, the previously reported BTTE without methoxy groups adopts an antiparallel conformation on account of the lack of widespread occurrence of intermolecular interactions.[8] Clearly, the methoxy group plays an important role in these crystals due to the presence of the electron-rich O atoms. Moreover, BTTA forms a twin crystal. The asymmetric nature of the twin crystal and cooperative intermolecular interactions finally lead BTTA to form a three-dimensional tubelike structure. Apparently, the variation in the six-membered ethene bridges from naphthalimide and benzothiadiazole to benzobisthiadiazole plays a key role in modulating intermolecular interactions, thus affecting the packing of these molecules.

Furthermore, the distance of the double bonds for central ethene bridges within naphthalimide (C3=C4), benzothiadiazole (C6=C11), and benzobisthiadiazole (C4=C5) are 1.398(2), 1.383(4), and 1.371(5) Å, respectively (Figures 6 and 7, and Figure S11 in the Supporting Information). Generally, the typical bond length is approximately 1.54 Å for a C−C single bond and 1.33 Å for a double bond. Among these three compounds, the relatively short bond length indicates that the bonding between C4−C5 in the BTTA system is nearer to a typical double bond. It is consistent

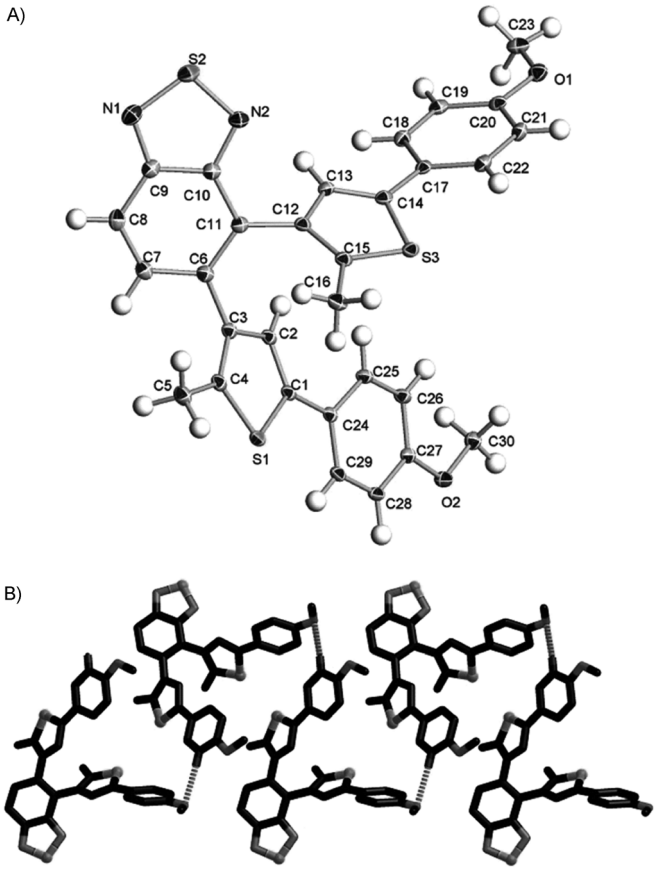

Figure 6. A) ORTEP representation of the crystal structure of BTA with displacement ellipsoids shown at the 25% probability level. Selected bond lengths [Å]: C6–C7 1.442(4), C10–C11 1.435(4), C6–C11 1.383(4). B) View of a linear structure formed by multiple C–H···O hydrogen bonds in the crystal of BTA.

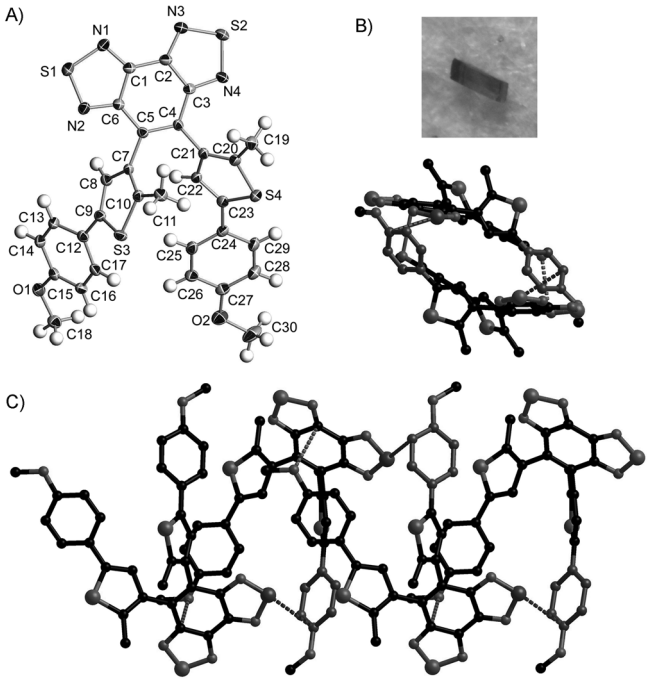

Figure 7. A) ORTEP representation of the crystal structure of BTTA with displacement ellipsoids shown at the 25% probability level. Selected bond lengths [Å]: C5–C6 1.452(5), C3–C4 1.454(5), C4–C5 1.371(5). B) Top view of a linear structure of BTTA formed by cooperative intermolecular S···C and O···C stacking interactions and a photographic image of a single crystal of BTTA obtained from slow evaporation of BTTA in a mixed solvent of $CHCl_3$–MeOH. C) Side view of the linear structure of BTTA. Hydrogen atoms are omitted for clarity. Selected atom distances [Å]: S···C 3.412(5), O···C 3.121(5).

with the aromaticity tendency: benzobisthiadiazole < benzothiadiazole < naphthalimide.

However, considering the good photochromic performance of BTE-NA, BTA, and BTTA in organic solvents, it is expected that the parallel arrangements in the single-crystal state can shift to the antiparallel conformation in solution due to the loss of the above-mentioned cooperative interactions in the well-ordered crystal state. Therefore, it is reasonable that the photochromic behavior can be distinctively different between the crystalline and solution phases. As illustrated by a further case (Figure S12 in the Supporting Information), BTE-NA, BTA, and BTTA also exhibit excellent photochromic properties and defined thermoreversible properties in an organogel system.[19] A stable gel with BTE-NA (1.66×10^{-3} wt%), BTA (1.28×10^{-3} wt%), and BTTA (1.59×10^{-3} wt%) dopants were formed around 20 w/w% Poloxamer 407 (Boluoshamu 407 with a molecular distribution of 9840–14600) in water, and showed an extraordinary sol–gel phase-transition temperature around 28°C (Figure S12 in the Supporting Information). Irradiation of the thermoreversible organogel with UV light at 365 nm leads to the appearance of new absorbance bands around 719 nm for BTE-NA, 655 nm for BTA, and 497 and 655 nm for BTTA, which could be bleached by irradiation with visible light at 575 nm.

Conclusion

Three compounds—BTE-NA, BTA, and BTTA, which contain electron-withdrawing groups of naphthalimide, benzothiadiazole, and benzobisthiadiazole as six-membered ring bridges—were specifically designed and synthesized. The three ethene bridges with different degrees of aromaticity could provide a systematical comparison in the thermal stability evolution of their corresponding closed forms. They show typical photochromic performance with considerably high cyclization quantum yields and high fatigue resistance in solution. The decrease in the aromaticity in ethene bridges was able to increase the thermal stability of the closed form at room temperature. c-BTE-NA shows first-order decay in various solvents, whereas c-BTA is only stable in nonpolar solvents. The lower aromaticity of BTTA gives rise to its unprecedented thermal stability in various solvents, even at elevated temperature in toluene. In a well-ordered crystal state, all three compounds adopt a parallel conformer, and BTTA forms a three-dimensional tubelike structure on account of the strong π···π stacking interactions and weak electrostatic interactions between the electron-

rich oxygen atom on the methoxy group and the carbon atom on the electron-deficient benzobisthiadiazole moiety. Furthermore, the fluorescence of BTE-NA, BTA, and BTTA could be modulated by photochromism and solvatochromism. This work contributes to the understanding of aromaticity-controlled thermal stability of the ethene bridge as well as novel building blocks for the photochromic BTE systems.

Experimental Section

General: ^{1}H and ^{13}C NMR spectra were recorded using Bruker AM-400 spectrometers with tetramethylsilane (TMS) as an internal reference. $CDCl_3$ and [D_6]benzene were used as solvents. HRMS spectra were recorded using a Waters LCT Premier XE spectrometer with methanol or acetonitrile as solvents. Absorption and fluorescence spectra were recorded using Varian Cary 500 and HORIBA Fluoromax 4 instruments, respectively. The photochromic reaction was induced in situ by continuous wavelength irradiation using an Hg/Xe lamp (Hamamatsu, LC8 Lightningcure, 200 W) equipped with narrow-band interference filters of appropriate wavelengths (Semrock Hg01 for $\lambda_{irr}=365$ nm, Semrock BrightLine FF01-575/25-25 for $\lambda_{irr}=575$ nm). The irradiation power was measured using a photodiode from Ophir (PD300-UV). The photochromic quantum yields were determined by probing the sample with a xenon lamp during the photochromic reaction. Absorption changes were monitored by a CCD camera mounted on a spectrometer (Ocean Optics). The fluorescence quantum yields were measured by the comparison of BTE-NA, BTA, and BTTA with standard 0.05 M quinine sulphate in sulfuric acid. 4-Bromo-*N*-butyl-3-iodo-1,8-naphthalimide,[11] 4,5-dibromo-2,1,3-benzothiadiazole,[12] 4,5-dibromobenzo[1,2-*c*:3,4-*c*′]bis-[1,2,5]thiadiazole,[8] and 5-(4-methoxyphenyl)-2-methylthiophen-3-ylboronic acid were prepared according to the established method.[12] All other reagents were of analytical purity and used without further treatment.

Synthesis of BTE-NA: 4-Bromo-*N*-butyl-3-iodo-1,8-naphthalimide (0.68 g, 1.5 mmol) was dissolved in dioxane (100 mL). Then [$Pd(PPh_3)_4$] (0.35 g) was added, and the resulting mixture was stirred for 15 min at room temperature. Then aqueous Na_2CO_3 (100 mL, 2.0 mol L^{-1}) was added. The reactive mixture was heated to reflux at a temperature of 60 °C, and the solution of 5-(4-methoxyphenyl)-2-methylthiophen-3-ylboronic acid (0.74 g, 3.0 mmol) was added dropwise with a syringe. Subsequently the mixture was heated to reflux for 24 h and cooled to room temperature. The reactive mixture was poured in H_2O and extracted with diethyl ether. The organic layer was separated and dried with Na_2SO_4. After concentration, the compound was purified by column chromatography on silica gel (CCl_4/ethyl acetate = 20:1 v/v) to yield a yellow solid (340 mg, yield: 35 %). ^{1}H NMR (400 MHz, $CDCl_3$): $\delta=0.98$ (t, $J=7.6$ Hz, 3H; $-CH_2CH_3$), 1.48–1.53 (m, 2H; $-CH_2CH_3$), 1.72–1.80 (m, 2H; $-NCH_2CH_2-$), 1.99 (s, 3H; $-CH_3$), 2.34 (s, 3H; $-CH_3$), 3.80 (s, 3H; $-OCH_3$), 3.84 (s, 3H; $-OCH_3$), 4.21 (t, $J=7.6$ Hz, 2H; $-NCH_2-$), 6.72 (s, 1H; thiophene-H), 6.81 (d, $J=8.8$ Hz, 1H; phenyl-H), 6.89 (d, $J=8.8$ Hz, 1H; phenyl-H), 6.97 (s, 1H; thiophene-H), 7.30 (d, $J=8.8$ Hz, 2H; phenyl-H), 7.44 (d, $J=8.8$ Hz, 2H; phenyl-H), 7.70 (t, $J=7.6$ Hz, 1H; naphthalene-H), 8.17 (d, $J=8.4$ Hz, 1H; naphthalene-H), 8.62 (d, $J=7.2$ Hz, 1H; naphthalene-H), 8.67 ppm (s, 1H; naphthalene-H); ^{1}H NMR (400 MHz, [D_6]benzene): $\delta=0.90$ (t, $J=7.6$ Hz, 3H; $-CH_2CH_3$), 1.39–1.45 (m, 2H; $-CH_2CH_3$), 1.82 (s, 3H; $-CH_3$), 1.87–1.93 (m, 2H; $-NCH_2CH_2-$), 2.13 (s, 3H; $-CH_3$), 3.22 (s, 3H; $-OCH_3$), 3.26 (s, 3H; $-OCH_3$), 4.36 (t, $J=7.2$ Hz, 2H; $-NCH_2-$), 6.69 (d, $J_1=8.4$ Hz, 2H; phenyl-H), 6.73 (d, $J_1=8.8$ Hz, 2H; phenyl-H), 6.84 (s, 1H; thiophene-H), 6.94 (s, 1H; thiophene-H), 7.40 (d, $J=8.4$ Hz, 2H; phenyl-H), 7.45 (d, $J=8.8$ Hz, 2H; phenyl-H), 7.99 (d, $J=8.4$ Hz, 1H; naphthalene-H), 8.63 (d, $J=6.8$ Hz, 1H; naphthalene-H), 8.91 ppm (s, 1H; naphthalene-H); ^{13}C NMR (100 MHz, $CDCl_3$): $\delta=13.91$, 14.06, 14.17, 20.45, 30.29, 40.33, 55.36, 55.41, 114.21, 114.35, 121.83, 122.83, 124.29, 125.09, 126.84, 126.93, 127.17, 127.21, 127.56, 130.92, 131.72, 133.07, 133.46, 134.57, 134.94, 135.73, 136.46, 137.38, 139.73, 139.94, 140.72, 158.98, 159.23, 164.08, 164.34 ppm; HRMS (TOF MS ESI$^+$): *m*/*z*: calcd for $C_{40}H_{36}NO_4S_2$: 658.2086 [*M*+H]$^+$; found: 658.2089.

Synthesis of BTA: BTA was prepared by a similar procedure to BTE-NA by Suzuki coupling between 4,5-dibromo-2,1,3-benzothiadiazole and 5-(4-methoxyphenyl)-2-methylthiophen-3-ylboronic acid (250 mg, yield: 57 %). ^{1}H NMR (400 MHz, $CDCl_3$): $\delta=2.07$ (s, 3H; $-CH_3$), 2.23 (s, 3H; $-CH_3$), 3.81 (s, 3H; $-OCH_3$), 3.82 (s, 3H; $-OCH_3$), 6.85–6.88 (m, 5H; phenyl-H), 7.04 (s, 1H; thiophene-H), 7.36 (d, $J=8.8$ Hz, 2H; phenyl-H), 7.42 (d, $J=8.8$ Hz, 2H; phenyl-H), 7.71 (d, $J=9.2$ Hz, 1H; phenyl-H), 8.02 ppm (d, $J=8.8$ Hz, 1H; phenyl-H); ^{1}H NMR (400 MHz, [D_6]benzene): $\delta=1.98$ (s, 3H; $-CH_3$), 2.03 (s, 3H; $-CH_3$), 3.22 (s, 3H; $-OCH_3$), 3.23 (s, 3H; $-OCH_3$), 6.68 (d, $J=6.0$ Hz, 2H; phenyl-H), 6.71 (d, $J=6.0$ Hz, 2H; phenyl-H), 6.95 (s, 1H; thiophene-H), 7.34 (d, $J=8.8$ Hz, 1H; phenyl-H), 7.44 (d, $J=8.8$ Hz, 2H; phenyl-H), 7.47 (d, $J=8.8$ Hz, 2H; phenyl-H), 7.79 ppm (d, $J=8.8$ Hz, 1H; phenyl-H); ^{13}C NMR (100 MHz, $CDCl_3$): $\delta=14.23$, 14.53, 55.37, 114.18, 114.27, 119.95, 124.30, 124.98, 126.83, 126.94, 127.10, 127.41, 128.27, 133.25, 133.76, 135.17, 136.59, 136.66, 137.46, 140.00, 140.16, 154.26, 155.16, 158.93, 159.06 ppm; HRMS (TOF MS ESI$^+$): *m*/*z*: calcd for $C_{30}H_{25}N_2O_2S_3$: 541.1078 [*M*+H]$^+$; found: 541.1078.

Synthesis of BTTA: BTTA was prepared by a similar procedure to BTE-NA by Suzuki coupling between 4,5-dibromobenzo[1,2-*c*:3,4-*c*′]bis-[1,2,5]thiadiazole and 5-(4-methoxyphenyl)-2-methylthiophen-3-ylboronic acid (270 mg, yield: 43 %). ^{1}H NMR (400 MHz, $CDCl_3$): $\delta=2.10$ (s, 3H; $-CH_3$, antiparallel conformer), 2.20 (s, 3H; $-CH_3$, parallel conformer), 3.81 (s, 3H; $-OCH_3$, parallel conformer), 3.83 (s, 3H; $-OCH_3$, antiparallel conformer), 6.84 (d, $J=8.4$ Hz, 2H; phenyl-H, parallel conformer), 6.88 (d, $J=8.8$ Hz, 2H; phenyl-H, antiparallel conformer), 6.92 (s, 1H; thiophene-H, parallel conformer), 7.13 (s, 1H; thiophene-H, antiparallel conformer), 7.38 (d, $J=8.8$ Hz, 2H; phenyl-H, parallel conformer), 7.44 ppm (d, $J=8.4$ Hz, 2H; phenyl-H, antiparallel conformer); ^{1}H NMR (400 MHz, [D_6]benzene): $\delta=1.98$ (s, 3H; $-CH_3$, antiparallel conformer), 2.04 (s, 3H; $-CH_3$, parallel conformer), 3.22 (s, 3H; $-OCH_3$, parallel conformer), 3.26 (s, 3H; $-OCH_3$, antiparallel conformer), 6.69 (d, $J=8.4$ Hz, 2H; phenyl-H, parallel conformer), 6.74 (d, $J=8.4$ Hz, 2H; phenyl-H, antiparallel conformer), 7.05 (s, 1H; thiophene-H, parallel conformer), 7.25 (s, 1H; thiophene-H, antiparallel conformer), 7.48 (d, $J=8.4$ Hz, 2H; phenyl-H, parallel conformer), 7.51 ppm (d, $J=8.8$ Hz, 2H; phenyl-H, antiparallel conformer); ^{13}C NMR (100 MHz, $CDCl_3$): $\delta=14.85$, 55.37, 114.24, 124.43, 124.57, 126.93, 127.03, 127.09, 130.75, 130.91, 132.42, 132.57, 137.07, 137.85, 140.33, 140.54, 147.48, 156.85, 157.15, 159.09 ppm; HRMS (TOF MS ESI$^+$): *m*/*z*: calcd for $C_{30}H_{22}N_4O_2S_4$: 598.0626 [*M*]$^+$; found: 598.0626.

Pure closed-form c-BTTA: BTTA was irradiated with UV light and separated on aluminum oxide eluted with CCl_4/dichloromethane (4:1 v/v). ^{1}H NMR (400 MHz, [D_6]benzene): $\delta=2.50$ (s, 6H; $-CH_3$), 3.19 (s, 6H; $-OCH_3$), 6.66 (d, $J=8.8$ Hz, 4H; phenyl-H), 7.64 (d, $J=8.8$ Hz, 4H; phenyl-H), 8.48 ppm (s, 2H; thiophene-H).

Photochromism of BTE-NA, BTA, and BTTA doped in thermosensitive organogel: The sol–gel system was based on commercially available Poloxamer 407 (Boluoshamu 407) with a molecular distribution of 9840–14600. The thermosensitive organogel with a dopant of BTE-NA, BTA, and BTTA was prepared as follows. A solution (200 μL) of BTE-NA (1.66×10^{-3} wt %), BTA (1.28×10^{-3} wt %), or BTTA (1.59×10^{-3} wt %) in THF was added to an aqueous solution of Poloxamer 407 (3.0 g; 20 % in weight ratio). The viscous solution was cooled to 5 °C and sonicated until the solution became transparent without obvious bubbles. The phase transition for thermosensitive organogel system was then about 28 °C. When keeping the temperature above 28 °C, Poloxamer 407 aqueous solution (20 % in weight ratio) became an organogel.

X-ray crystallography for BTE-NA: $C_{40}H_{35}NO_4S_2$; $M_r=657.81$ g mol^{-1}; yellow block; $0.35\times0.15\times0.05$ mm^3; triclinic; space group $P\bar{1}$; $a=11.4898(12)$, $b=11.9884(13)$, $c=14.1549(15)$ Å; $F(000)=692.0$; $\rho_{calcd}=1.342$ g mol^{-1}; $\mu(Mo_{K\alpha})=0.208$; $T=133$ K; 12582 measured reflections, 7033 unique reflections ($R_{int}=0.0296$), 5972 with $I\geq2\sigma(I)$ used in refine-

ment, final $wR_2 = 0.1434$, R_1 ($I > 2\sigma(I)$) $= 0.0416$; GoF $= 1.088$; largest final difference peak/hole $= +0.43/-0.35$ e Å^{-3}.

X-ray crystallography for BTA: $C_{30}H_{24}N_2O_2S_3$; $M_r = 540.69$ g mol^{-1}; yellow block; $0.40 \times 0.20 \times 0.18$ mm^3; monoclinic; space group $P2_1/n$; $a = 7.5004(9)$, $b = 28.647(3)$, $c = 12.1653(14)$ Å; $F(000) = 1128.0$; $\rho_{calcd} = 1.375$ g mol^{-1}; $\mu(Mo_{K\alpha}) = 0.316$; $T = 133$ K; 19898 reflections measured using a Bruker SMART Apex diffractometer, of which 5698 ($R_{int} = 0.0307$), 19898 measured reflections, 5698 unique reflections ($R_{int} = 0.0307$), 4963 with $I \geq 2\sigma(I)$ used in refinement, final $wR_2 = 0.1435$, R_1 ($I > 2\sigma(I)$) $= 0.0533$; GoF $= 1.158$; largest final difference peak/hole $= +0.574/-0.448$ e Å^{-3}.

X-ray crystallography for BTTA: $C_{30}H_{22}N_4O_2S_4$; $M_r = 598.76$ g mol^{-1}; Kelly block; $0.23 \times 0.11 \times 0.09$ mm^3; triclinic; space group $P\bar{1}$; $a = 12.301(4)$, $b = 12.559(4)$, $c = 19.099(6)$ Å; $F(000) = 1240.0$; $\rho_{calcd} = 1.426$ g mol^{-1}; $\mu(Mo_{K\alpha}) = 0.377$; $T = 298$ K; 13570 measured reflections, 9518 unique reflections ($R_{int} = 0.0306$), 5763 with $I \geq 2\sigma(I)$ used in refinement, final $wR_2 = 0.1362$, R_1 ($I > 2\sigma(I)$) $= 0.0518$; GoF $= 1.011$; largest final difference peak/hole $= +0.216/-0.220$ e Å^{-3}.

Structure solution of BTE-NA, BTA, and BTTA was carried out by direct methods and full-matrix least-squares refinement against F^2 (all data) using SHELXTL.[20] Hydrogen atoms bound to C were placed at calculated positions.

CCDC-862019 (BTE-NA), 862020 (BTA), and 862021 (BTTA) contain the supplementary crystallographic data for this paper. These data can be obtained free of charge from The Cambridge Crystallographic Data Centre via www.ccdc.cam.ac.uk/data_request/cif.

Acknowledgements

This work was supported by the NSFC of China, the National 973 Program (2011CB808400), the Oriental Scholarship, SRFDP (200802510011 and 20100074110015), the Program for New Century Excellent Talents in University (NCET), the Innovation Program of Shanghai Municipal Education Commission, and the Fundamental Research Funds for the Central Universities (WK1013002).

[1] a) R. A. Evans, T. L. Hanley, M. A. Skidmore, T. P. Davis, G. K. Such, L. H. Yee, G. E. Ball, D. A. Lewis, *Nat. Mater.* **2005**, *4*, 249–253; b) H. Tian, Y. L. Feng, *J. Mater. Chem.* **2008**, *18*, 1617–1622; c) J. Andréasson, U. Pischel, *Chem. Soc. Rev.* **2010**, *39*, 174–188; d) B. L. Feringa, *Molecular Switches*, Wiley-VCH, Weinheim, Germany, **1990**; e) F. M. Raymo, M. Tomasulo, *Chem. Soc. Rev.* **2005**, *34*, 327–336; f) H. D. Samachetty, N. R. Branda, *Pure Appl. Chem.* **2006**, *78*, 2351–2359; g) T. Darwish, R. Evans, M. James, N. Malic, G. Triani, T. Hanley, *J. Am. Chem. Soc.* **2010**, *132*, 10748–10755; h) L. Zhu, M. Zhu, J. Hurst, A. D. Q. Li, *J. Am. Chem. Soc.* **2005**, *127*, 8968–8970; i) Z. Y. Tian, W. W. Wu, A. D. Q. Li, *ChemPhysChem* **2009**, *10*, 2577–2591; j) J. Andréasson, S. D. Straight, T. A. Moore, A. L. Moore, D. Gust, *J. Am. Chem. Soc.* **2008**, *130*, 11122–11128; k) H. Tian, *Angew. Chem.* **2010**, *122*, 4818–4820; *Angew. Chem. Int. Ed.* **2010**, *49*, 4710–4712.

[2] a) M. Irie, *Chem. Rev.* **2000**, *100*, 1685–171; b) A. Spangenberg, R. Métivier, J. Gonzalez, K. Nakatani, P. Yu, M. Giraud, A. Léaustic, R. Guillot, T. Uwada, T. Asahi, *Adv. Mater.* **2009**, *21*, 309–313; c) A. Spangenberg, A. Brosseau, R. Métivier, M. Sliwa, K. Nakatani, T. Asahi, T. Uwada, *J. Phys. Org. Chem.* **2007**, *20*, 985–991; d) P. Remón, M. Bälter, S. M. Li, J. Andréasson, U. Pischel, *J. Am. Chem. Soc.* **2011**, *133*, 20742–20745; e) G. Y. Jiang, Y. L. Song, X. F. Guo, D. Q. Zhang, D. B. Zhu, *Adv. Mater.* **2008**, *20*, 2888–2898; f) S. Yamamoto, K. Matsuda, M. Irie, *Angew. Chem.* **2003**, *115*, 1674–1677; *Angew. Chem. Int. Ed.* **2003**, *42*, 1636–1639.

[3] a) H. Tian, B. Z. Chen, H. Y. Tu, K. Müllen, *Adv. Mater.* **2002**, *14*, 918–923; b) T. Yamaguchi, M. Irie, *J. Mater. Chem.* **2006**, *16*, 4690–4694; c) T. Nakashima, K. Atsumi, S. Kawai, T. Nakagawa, Y. Hasegawa, T. Kawai, *Eur. J. Org. Chem.* **2007**, 3212–3218; d) K. Yagi, M. Irie, *Bull. Chem. Soc. Jpn.* **2003**, *76*, 1625–1628; e) S. Z. Pu, G. Liu, L. Shen, J. K. Xu, *Org. lett.* **2007**, *9*, 2139–2142; f) Y. Wu, S. J. Chen, Y. H. Yang, Q. Zhang, Y. S. Xie, H. Tian, W. H. Zhu, *Chem. Commun.* **2012**, *48*, 528–530.

[4] a) B. Gorodetsky, N. R. Branda, *Adv. Funct. Mater.* **2007**, *17*, 786–796; b) H. Tian, B. Z. Chen, H. Liu, *Chem. Lett.* **2001**, *30*, 990–991; c) M. Ohsumi, T. Fukaminato, *Chem. Commun.* **2005**, 3921–3923.

[5] a) V. W. W. Yam, C. C. Ko, N. Zhu, *J. Am. Chem. Soc.* **2004**, *126*, 12734–12735; b) C. C. Ko, W. M. Kwok, V. W. W. Yam, D. L. Phillips, *Chem. Eur. J.* **2006**, *12*, 5840–5848.

[6] K. Suzuki, T. Ubukata, Y. Yokoyama, *Chem. Commun.* **2012**, *48*, 765–767.

[7] S. Nakamura, M. Irie, *J. Org. Chem.* **1988**, *53*, 6136–6138.

[8] W. Zhu, Y. H. Yang, R. Métivier, Q. Zhang, R. Guillot, Y. S. Xie, H. Tian, K. Nakatani, *Angew. Chem.* **2011**, *123*, 11178–11182; *Angew. Chem. Int. Ed.* **2011**, *50*, 10986–10990.

[9] a) W. H. Zhu, Y. Z. Wu, S. T. Wang, W. Q. Li, X. Li, J. Chen, Z. S. Wang, H. Tian, *Adv. Funct. Mater.* **2011**, *21*, 756–763; b) Q. Zou, H. Tian, *Sens. Actuators B* **2010**, *149*, 20–27; c) C. M. Zhong, C. H. Duan, F. Huang, H. B. Wu, Y. Cao, *Chem. Mater.* **2011**, *23*, 326–340; d) S. H. Chen, Y. J. Li, W. L. Yang, N. Chen, H. B. Liu, Y. L. Li, *J. Phys. Chem. C* **2010**, *114*, 15109–15115; e) L. J. Zhang, C. He, J. W. Chen, P. Yuan, L. Huang, C. Zhang, W. Z. Cai, Z. T. Liu, Y. Cao, *Macromolecules* **2010**, *43*, 9771–9778; f) C. Li, M. Y. Liu, N. G. Pschirer, M. Baumgarten, K. Müllen, *Chem. Rev.* **2010**, *110*, 6817–6855; g) X. H. Qian, Y. Xiao, Y. F. Xu, X. F. Guo, J. H. Qian, W. P. Zhu, *Chem. Commun.* **2010**, *46*, 6418–6436.

[10] J. R. Lakowicz, *Principles of Fluorescence Spectroscopy*, Springer, **2006**, pp. 209–216.

[11] X. L. Meng, W. H. Zhu, Q. Zhang, Y. L. Feng, W. J. Tan, H. Tian, *J. Phys. Chem. B* **2008**, *112*, 15636–15645.

[12] W. H. Zhu, X. L. Meng, Y. H. Yang, Q. Zhang, Y. S. Xie, H. Tian, *Chem. Eur. J.* **2010**, *16*, 899–906.

[13] A. Komin, M. Carmack, *J. Heterocycl. Chem.* **1975**, *12*, 829–833.

[14] S. H. Kawai, S. L. Gilat, R. Ponsinet, J. L. Lehn, *Chem. Eur. J.* **1995**, *1*, 285–293.

[15] C. C. Ko, L. X. Wu, K. M. C. Wong, N. Y. Zhu, V. W. W. Yam, *Chem. Eur. J.* **2004**, *10*, 766–776.

[16] Gaussian 09, Revision A.02, M. J. Frisch, G. W. Trucks, H. B. Schlegel, G. E. Scuseria, M. A. Robb, J. R. Cheeseman, G. Scalmani, V. Barone, B. Mennucci, G. A. Petersson, H. Nakatsuji, M. Caricato, X. Li, H. P. Hratchian, A. F. Izmaylov, J. Bloino, G. Zheng, J. L. Sonnenberg, M. Hada, M. Ehara, K. Toyota, R. Fukuda, J. Hasegawa, M. Ishida, T. Nakajima, Y. Honda, O. Kitao, H. Nakai, T. Vreven, J. A. Montgomery, Jr., J. E. Peralta, F. Ogliaro, M. Bearpark, J. J. Heyd, E. Brothers, K. N. Kudin, V. N. Staroverov, R. Kobayashi, J. Normand, K. Raghavachari, A. Rendell, J. C. Burant, S. S. Iyengar, J. Tomasi, M. Cossi, N. Rega, J. M. Millam, M. Klene, J. E. Knox, J. B. Cross, V. Bakken, C. Adamo, J. Jaramillo, R. Gomperts, R. E. Stratmann, O. Yazyev, A. J. Austin, R. Cammi, C. Pomelli, J. W. Ochterski, R. L. Martin, K. Morokuma, V. G. Zakrzewski, G. A. Voth, P. Salvador, J. J. Dannenberg, S. Dapprich, A. D. Daniels, O. Farkas, J. B. Foresman, J. V. Ortiz, J. Cioslowski, D. J. Fox, Gaussian, Inc., Wallingford CT, **2009**.

[17] C. Adamo, V. Barone, *J. Chem. Phys.* **1999**, *110*, 6158–6170.

[18] E. Cancès, B. Mennucci, J. Tomasi, *J. Chem. Phys.* **1997**, *107*, 3032–3041.

[19] a) J. C. Wu, T. Yi, T. M. M. X. Yu, Z. G. Zhou, M. Xu, Y. F. Zhou, H. J. Zhang, J. T. Han, F. Y. Li, C. H. Huang, *Angew. Chem.* **2008**, *120*, 1079–1083; *Angew. Chem. Int. Ed.* **2008**, *47*, 1063–1067; b) S. A. M. Ahmed, J. L. Pozzo, *J. Photochem. Photobiol. A* **2008**, *200*, 57–67.

[20] G. M. Sheldrick, SHELXS 97 and SHELXL 97, Programs for Crystal Structure Solution and Refinement, University of Göttingen, Göttingen, Germany **1997**.

Received: February 2, 2012
Revised: May 9, 2012
Published online: August 2, 2012

